



**HAL**  
open science

## Microfluidically Tunable Microstrip Filters

Daouda Lamine Diedhiou, Ronan Sauleau, Artem V. Boriskin

► **To cite this version:**

Daouda Lamine Diedhiou, Ronan Sauleau, Artem V. Boriskin. Microfluidically Tunable Microstrip Filters. IEEE Transactions on Microwave Theory and Techniques, 2015, 63 (7), pp.2245–2252. 10.1109/TMTT.2015.2435704 . hal-01240767

**HAL Id: hal-01240767**

**<https://univ-rennes.hal.science/hal-01240767>**

Submitted on 4 Jan 2016

**HAL** is a multi-disciplinary open access archive for the deposit and dissemination of scientific research documents, whether they are published or not. The documents may come from teaching and research institutions in France or abroad, or from public or private research centers.

L'archive ouverte pluridisciplinaire **HAL**, est destinée au dépôt et à la diffusion de documents scientifiques de niveau recherche, publiés ou non, émanant des établissements d'enseignement et de recherche français ou étrangers, des laboratoires publics ou privés.

# Microfluidically Tunable Microstrip Filters

D.L. Diedhiou, R. Sauleau, *Senior Member, IEEE*, and A.V. Boriskin, *Senior Member, IEEE*

**Abstract**— A new approach for the development of tunable and reconfigurable microstrip devices is proposed. The basic idea consists in using a suspended substrate with integrated network of plastic tubes, which can be selectively filled in with a high permittivity dielectric fluid, e.g. water. The local change of the substrate effective permittivity achieved in such a way enables one to change, in a controlled and reversible manner, the electrical length of certain elements of microstrip circuits. As a proof-of-concept, tunable stub resonators based on suspended and inverted microstrip lines are designed and characterized in frequency and time domains. Then, the same principle is applied for the development of a 4th-order bandpass filter with 40% fractional bandwidth operating at 5 GHz. A tunable range of 19.5% with the insertion loss of 0.6 dB is demonstrated. The performance of the stub resonators and filter is validated successfully via prototyping.

**Index Terms**— Dielectric fluid, microfluidics, reconfigurable, suspended microstrip line, tunable filters.

## I. INTRODUCTION

THE new generation of communication systems strongly relies on reconfigurable devices enabling multiband operations. In this context, an extensive research has been done on agile devices and especially on bandpass filters. Reconfigurable and tunable filters are among the key components for emerging wideband and multifunctional RF front-ends. Nowadays, there are several techniques available for developing tunable filters with very good performance characteristics, including microelectromechanical systems (MEMS) [1]-[3], PIN diodes [4], varactors [5], [6], and agile materials [7]-[9]. These established approaches enable development of very compact, cheap and robust tunable filters with fast switching time. However, tunable filters based on these approaches may have certain limitations such as the insufficient long-term reliability due to mechanical strength at small dimensions intrinsic to MEMS, power consumption in case of PIN diodes, and insertion loss intrinsic for varactor diodes and agile materials [10]. The risk of an electrical breakdown for electrically-controlled tunable devices can also limit their applicability for some high-power applications.

Microfluidic tunable devices propose an interesting alternative route to investigate. Instead of using electrical switches, they rely on the use of small volumes of conductive or dielectric fluids, whose flow is controlled by a micropump or external stimuli. A precise and reversible manipulation with the shape or position of fluid droplets enables development of various tunable microwave devices, including phase shifters [11], filters [12]-[16], MEMS [17], [18], and unit cells for frequency selective surfaces [19] and transmit arrays [20].

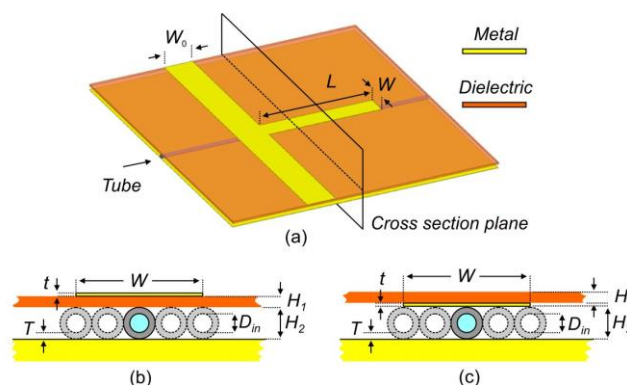


Fig. 1. Geometry and notations of a microstrip stub resonator with a dielectric tube placed below the suspended substrate: (a) 3-D view, (b, c) Cross-sectional views of the stub resonator based on the suspended and inverted microstrip lines, respectively.

In this paper, we introduce a new approach for the development of tunable filters based on microfluidic principle and animated using dielectric fluids (Fig. 1). The basic idea of this approach was introduced in [12] in the form of a tunable stub resonator backed on to a polymer substrate with integrated microfluidic channels. In [15], a cavity-backed microfluidically switchable filter animated using two different fluids was reported.

Manuscript received 17/12/2014.

This work was supported by Region Bretagne under the LiMA project.

D.L. Diedhiou, R. Sauleau, and A.V. Boriskin are with the Institut d'Electronique et de Télécommunications de Rennes (IETR), UMR CNRS 6164, Dept. of Antennas and Microwaves, Université de Rennes 1, Rennes, France (e-mails: artem.boriskin@ieee.org).

Unlike earlier studies [12], [15], the microfluidic network of the filters reported in the current paper is created using plastic tubes placed below a suspended dielectric substrate supporting inverted microstrip lines oriented along the stubs. The specific orientation of the microfluidic channels and the use of commercially-available materials helped us to increase the filter tuning range and simplify its practical implementation. The advantages of this approach compared to the cavity-based filter reported in [15] include lower complexity of the microfluidic network, proven reversible performance, faster switching time, and lower insertion loss. Finally, the flexibility of plastic tubing potentially enables their integration into conformal and flexible substrates, which is not the case for the designs reported in [12], [15]. This makes the proposed approach potentially compatible with emerging applications in the domain of flexible electronics, such as body-worn wireless sensors for medical and robotic applications.

The paper is organized as follows. The concept of the tunable stub resonator based on suspended and inverted microstrip lines is presented in Section II. Then, a 4th-order ultra-wideband (UWB) bandpass filter is reported Section III. Finally, conclusions are summarized in Section IV.

## II. MICROFLUIDICALLY TUNABLE STUB RESONATORS

### A. The stub topology, Materials, and Methods

The topology of the proposed quarter-wave tunable stub resonator is shown in Fig. 1. Two alternative configurations based on suspended (Fig. 1b) and inverted (Fig. 1c) microstrip (MS) lines are considered. The resonators are designed on the Rogers RT/Duroid 5880 substrate ( $H_1 = 0.254$  mm,  $\epsilon_r = 2.2$ ,  $\tan\delta = 0.0009$  at 10 GHz) with a standard copper cladding ( $t = 18\mu\text{m}$ ). For the suspended configuration (Fig. 1b), the use of thin laminate helps us to enhance the impact produced by a small volume of water guided by tubes. On the contrary, for the inverted MS line (Fig. 1c), the substrate thickness is less important because the fields are mostly confined in free space. For consistency, both resonators are initially designed on the same substrate.

The signal line width for the suspended and inverted MS lines is equal to  $W_0 = 3.2$  mm and 2.4 mm, respectively, which provides a  $50\ \Omega$  characteristic impedance in both cases. The central frequency of the resonators is set at 5 GHz.

The size of the air gap between the ground plane and the suspended substrate (or the strip in case of the inverted MS line) is defined as  $H_2 = D_{out} = 0.5$  mm, where  $D_{out}$  is the external diameter of the ultrathin-wall PTFE tube from AdTech, UK (this selection is based on the availability, however, it fits well the size of the air gap required for suspended microstrip circuits operating in the addressed frequency band). The permittivity and loss tangent of the tube material are  $\epsilon_r = 2.1$  and  $\tan\delta = 0.0004$  at 10 GHz. The tube internal diameter is  $D_{in} = 0.3$  mm.

The fluid used in this study is deionized (DI) water, whose permittivity at 5 GHz is defined as  $\epsilon_r = 74$ ,  $\tan\delta = 0.3$ . These values are given by the Debye function at 25°C [21], [22]. The large value of the water permittivity results in a significant local change of the substrate effective permittivity even for a small volume of water guided by the tube. This effect can be further enhanced using several tubes. Note that the tube diameter is only a fraction of the strip width, so several tubes can be placed under the stub simultaneously (Fig. 1b and 1c).

The electromagnetic performance of the devices reported in this paper is studied using the full-wave commercial software HFSS v.15 based on the finite element method.

### B. Simulation data

The width of MS lines affects the substrate effective permittivity and thus Q-factor and resonant frequency of the stub resonators. The freedom in selection of the stub width can be used to enhance its tuning range. This effect is illustrated in Fig. 2 which shows the frequency response of the stub resonators having different width ( $W = 1$  mm and 2 mm) with one tube placed below the substrate. The length of the stubs is given in the figure legends.

As we can see in Fig. 2, the narrower stub demonstrates a stronger shift of the resonant frequency between the 'on' and 'off' states, which correspond to the tube with and without water, respectively. We can also see that the stub resonator based on the inverted MS line has better agility than the one based on the suspended line. Both observations are explained by the ratio of volumes occupied by the tube and by the electric fields of the MS line. The larger the ratio, the stronger impact on the effective permittivity (and thus agility of the resonant frequency) is observed.

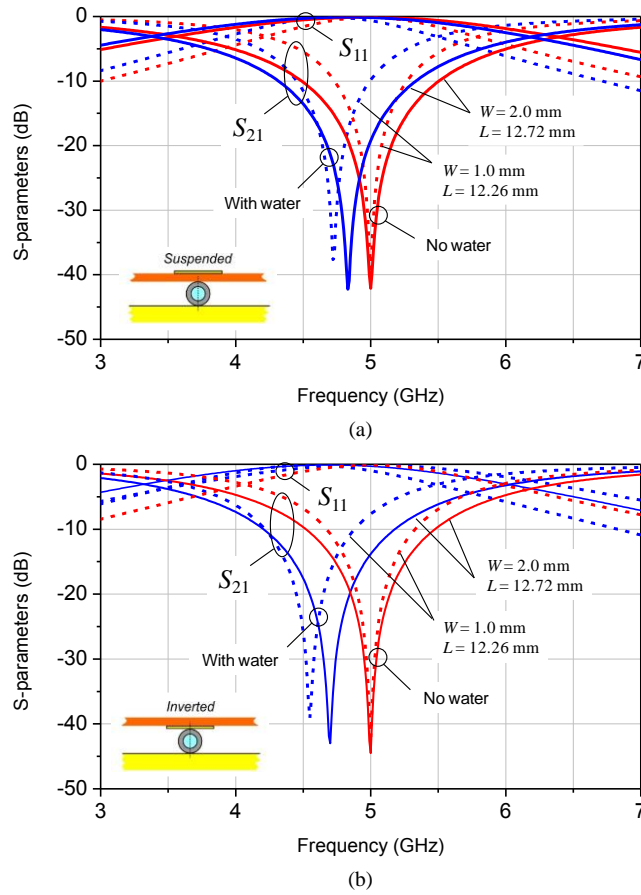


Fig. 2. Simulated S-parameters of the the suspended (a) and inverted (b) stub resonators with one tube placed under the stubs as shown in inset: (green line) no water, (blue line) with water. Different styles of the lines denote the stubs with different width: (dashed line)  $W = 1$  mm, (solid line)  $W = 2$  mm.

As we can see in Fig. 3, the tuning range can be further expanded by increasing the number of tubes,  $N$ . For each value of  $N$ , the frequency shift (tuning range) is determined as follows:

$$\Delta f = (f_1 - f_2)/f_1, \quad (1)$$

where  $f_1$  and  $f_2$  is the stub resonant frequency without and with water, respectively, defined from HFSS simulations. Note that  $f_1 > f_2$ . Again, the response is studied for inverted and suspended stub resonators having width of  $W = 1$  and  $2$  mm. The black triangular marks indicate the values of  $N$  for which the area covered with tubes equals the stub width, namely  $N \times D_{\text{out}} = W$ .

For the narrower stubs ( $W = 1$  mm), the frequency shift  $\Delta f$  grows rapidly for  $N$  ranging from 1 to 3 and reaches about 11% and 17% for the suspended and inverted MS lines, respectively. On the contrary, for the wider stubs ( $W = 2$  mm)  $\Delta f$  grows slower but reaches higher values of about 14% and 20%, respectively. The stronger agility observed for wide stubs and those based on inverted MS lines is explained by the larger relative variation of the substrate effective permittivity (Fig. 4). Here, the effective permittivity is estimated as

$$\epsilon_{\text{eff}}(N) = [c/(4(L+\Delta L) \times f_N)]^2, \quad (2)$$

where  $c$  is the speed of light in vacuum,  $L$  is the physical length of the stub,  $\Delta L$  is the equivalent length of the open stub due to the fringing fields [23], and  $f_N$  is the stub resonant frequency taken from HFSS data for a given number of tubes. Here, we assume that  $\Delta L$  does not depend on  $N$  and thus can be defined analytically for  $N = 0$ . This assumption does not take into account the variation of the charge in fringing profile, however this effect is minor and thus can be neglected.

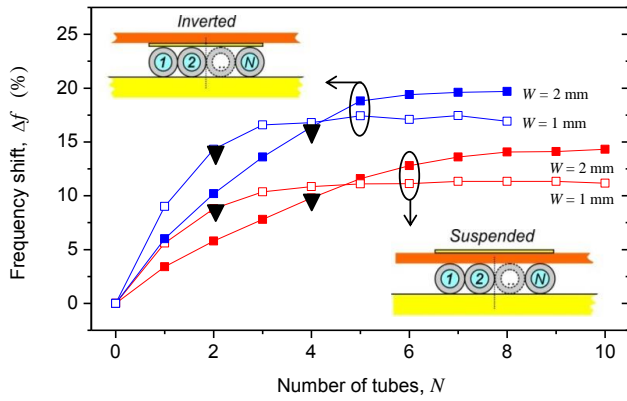


Fig. 3. Shift of the resonator frequency of the stub resonators vs. number of tubes. Two pairs of curves correspond to the stubs based on the inverted (blue line) and suspended (red line) MS lines. The hollow and solid rectangular marks denote the stubs with  $W = 1$  mm and  $2$  mm, respectively. The triangular marks indicate the values of  $N$  for which the tube area is equal to the width of the stub.

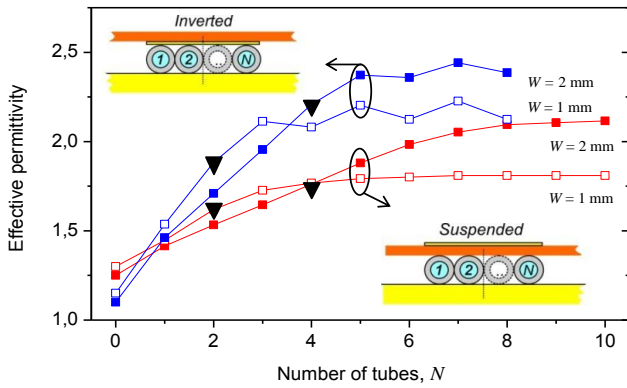


Fig. 4. Effective permittivity of the substrate calculated according to Eqn. (2) vs. number of tubes. The notations are the same as in Fig. 3.

The comparison of Fig. 3 and 4 reveals that the maximum tuning range is achieved when tubes cover the area with the width of approximately  $2W$ . A further increase of  $N$  produces no impact in terms of the frequency shift. The ripples observed for inverted stubs in Fig. 4 for  $N > 3$  are due to positioning of the tubes with respect to the stub central line for odd and even values of  $N$ . The tubes are always centered with respect to the stub, thus for  $N$  odd and even the stub edges occur either above the center of the tube (inset Fig. 1) or between the tubes (inset Fig. 4).

The impact of the tube material is studied in Fig. 5 for the case of one centered tube, whose permittivity,  $\epsilon_t$ , is varied from  $\epsilon_t = 1$  to  $20$ . For each value of  $\epsilon_t$ , the frequency shift is determined with respect to the resonant frequency of the stub with an empty tube having the same permittivity value. The dimensions of the tube remain constant. As we can see, the tuning range increases rapidly when  $\epsilon_t$  varies from  $1$  to  $5$ . Further increase leads to a monotonic decrease of  $\Delta f$  because the higher permittivity of the tube material reduces the variation of the substrate effective permittivity achieved due to water. This tendency is similar for both structures, however, a twofold advantage in terms of tuning range is observed for the inverted MS line.

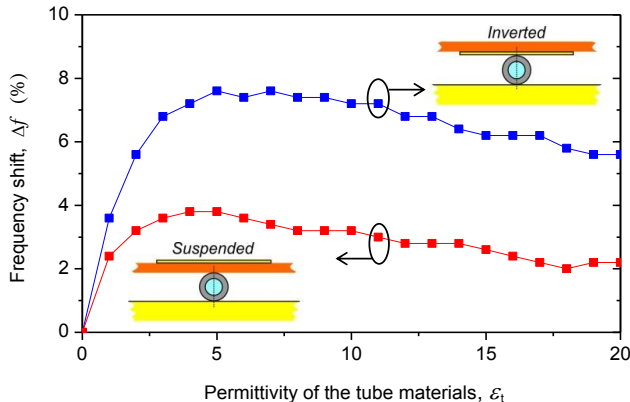


Fig. 5. Shift of the resonant frequency for the stub resonators ( $W = 2$  mm) based on the inverted ( $L = 12.72$  mm) and suspended ( $L = 12.85$  mm) MS lines vs. permittivity of the tube material.

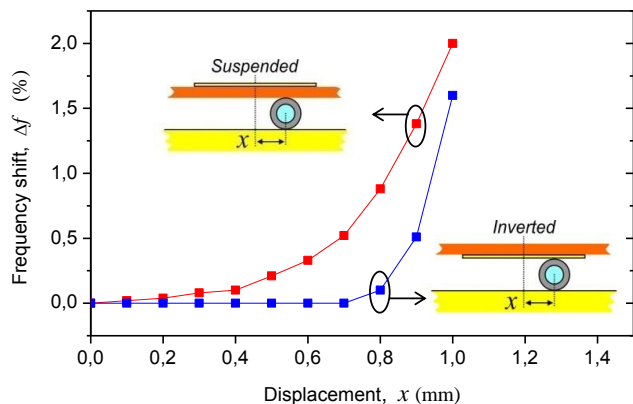


Fig. 6. Shift of the resonant frequency for the stub resonators ( $W = 2$  mm) based on the inverted ( $L = 12.72$  mm) and suspended ( $L = 12.85$  mm) MS lines vs. tube displacement with respect to the stub central line.

Finally, the impact of the tube position on the stub resonant frequency is illustrated in Fig. 6. The tube is filled with water. For each point, the frequency shift is determined with respect to the resonant frequency of the same stub with a centered tube. As we can see, the inverted stub is less sensitive to the misalignment than the suspended one. Indeed, a nearly zero frequency shift is observed for the inverted MS line until the tube is located underneath the strip. On the opposite, the resonant frequency of the suspended stub slowly varies even for a minor shift of the tube with respect to the central position ( $x \geq 0.2$  mm). This analysis is important because of two reasons. First, it gives information about the possible errors due to the tube misalignment in the proof-of-concept experimental studies reported below. Second, it reveals immunity of the inverted stubs to the positioning of the microfluidic network, whose architecture, in some cases, is predetermined by the structure of the substrate, e.g. [12].

### C. Experimental data (frequency domain)

To verify experimentally the feasibility of the proposed approach, several prototypes of microfluidic tunable stub resonators (both suspended and inverted) have been fabricated. However, for brevity, we limit the following discussion to the structures based on inverted MS lines.

Fig. 7 shows a prototype of the microfluidic tunable stub resonator fabricated by laser etching. A 6mm-thick aluminum plate is used as a support and ground plane. Circular washers with a thickness of 0.5 mm keep the substrate suspended above the ground plane. The tube is placed below the printed circuit board (PCB) and aligned with respect to the notches cut on the edge of the PCB (Fig. 7a). The water is supplied by a numerically controlled ElveFlow<sup>®</sup> pressure generator enabling a stable pulseless flow with a possible modulation of the pressure in time.

To prevent the substrate bending, the stub is fabricated on 1 mm thick Rogers RT/Duroid 5880 laminate. The use of the thicker substrate led to a minor shift of the central frequency that was compensated by adjusting the length of the stub.

The measurements are performed using the Agilent N5242A PNA-X Vector Network Analyzer through standard SMA connectors with flat center conductors.

Fig. 8 compares the simulated and measured S-parameters of the stub resonator shown in Fig. 7 with one and two tubes. As a reference, the frequency response of the same stub with empty tubes is also shown. As we can see, a good agreement between the measured and simulated data is obtained for both configuration. A minor discrepancy observed for 'on' state (with water) can be attributed to (i) inaccuracy in the definition of the water permittivity, (ii) inaccuracy in the definition of the tube materials properties, and (iii) imperfect shape of the tube core. The former factor may occur due to the temperature relation of the water permittivity and the bounded water phenomenon, which alters the permittivity of water in narrow capillaries. The other two factors come from the fabrication quality. Microscopic images of the tube revealed the imperfect circular shape of the tube core, which may result in some fluctuation of the volume of water inside the tube. As a consequence, local variation of the effective permittivity is also possible. The tube material properties were not studied due to very small dimensions, although this parameter can strong affect the response (see Fig. 5).

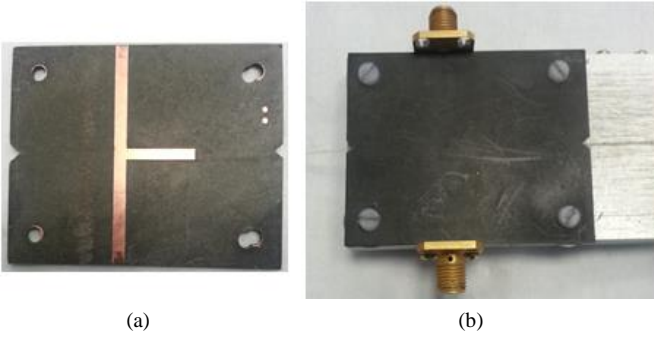


Fig. 7. Prototype of the inverted stub resonator ( $W = 2 \text{ mm}$ ,  $L = 12.85 \text{ mm}$ ,  $H_1 = 1 \text{ mm}$ ): (a) PCB plate with a microstrip stub resonator, (b) assembled device with SMA connectors and one tube placed underneath the PCB plate.

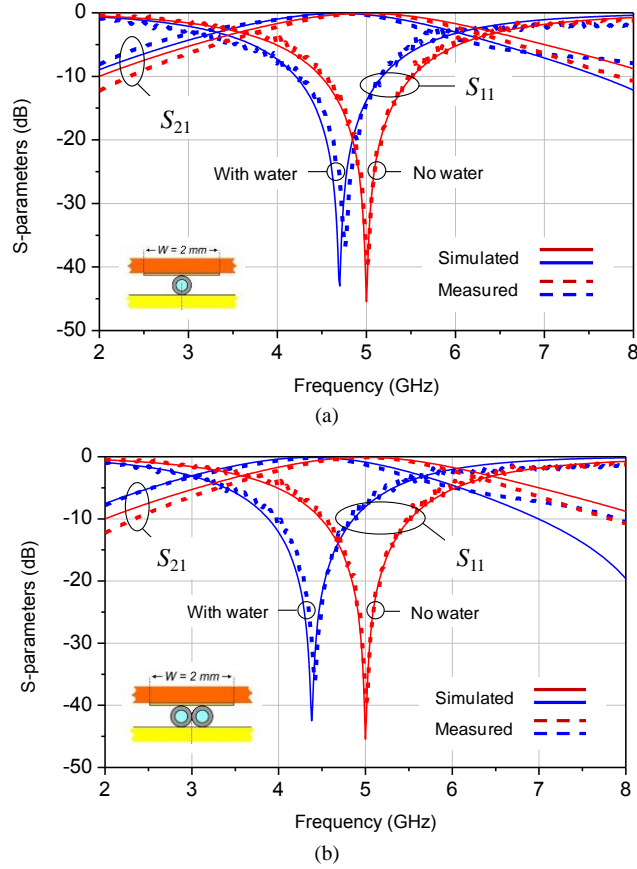


Fig. 8. Simulated (solid line) and measured (dashed line) S-parameters for the stub resonator Shown in Fig. 7: (a) one tube, (b) two tubes.

#### D. Experimental data (time domain)

To assess the switching time of the microfluidic tunable devices, a setup illustrated in Fig. 9a with two pressure generators (PG) was developed. Here, PG1 was used to provide a constant air flow with a pressure  $p_0 \sim 400 \text{ mbar}$ , whereas PG2 was providing a water flow with the pressure of  $p = p_0 \pm 200 \text{ mbar}$  modulated in time. The modulation period was 2s with a low pressure provided for 0.5s. The device under test (DUT) is the single stub resonator shown in Fig. 7 with 1 tube, whose frequency response is shown in Fig. 8a. The S-parameters of the stub resonator measured at the central frequency in time domain are illustrated in Fig. 9b. The high and low level of  $S_{11}$  corresponds to the 'on' and 'off' states of the device. The time sweep is 180s with a break from 6s to 174s. As we can see, the level and pulse duration of  $S_{11}$  remains stable with time. The switching time is estimated as  $t_s = 70\text{ms} \pm 20\text{ms}$  (this estimate is based on the roll-off time of the  $S_{11}$  impulse).

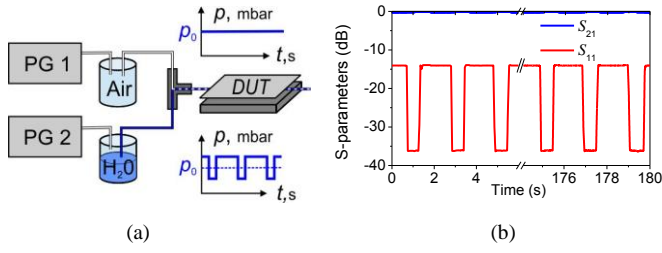


Fig. 9. Time domain measurements of the stub resonator presented in Fig. 7: (a) schematic drawing of the experimental setup with two pressure generators providing a stable airflow and pulse water flow mixed in the T-junction, (b) S-parameters measured in time domain at the central frequency.

### III. MICROFLUIDICALLY TUNABLE BANDPASS FILTER

#### A. Filter topology & Simulation data

The topology of the proposed microfluidic tunable bandpass filter is shown in Fig. 10. The filter consists of four half-wave tunable stub resonators separated by quarter-wave inverters. The synthesis of the filter is based on the Tchebycheff approximation [23]. The dimensions of the proposed filter are given in Table I. The 'initial' dimensions are obtained for the filter with no tubes. The 'optimized' ones are determined in an additional optimization step taking into account the presence of one tube filled with water. This additional step enabled us to achieve the desired -20 dB level of the reflection coefficient for all states of the filter, namely with one and two tubes with and without water (Fig. 11). The central frequency of the filter in 'off' state,  $f_1$ , is set as 5 GHz. The -3dB fractional bandwidth (FBW) is 40% for all states. The filter tuning range  $\Delta f$  equals 8% and 12% for one and two tubes, respectively, if defined in accordance with Eqn. (1), where  $f_1$  and  $f_2$  is the central frequency of the filter in 'off' and 'on' states, respectively. For both states, the central frequency is defined as the geometric mean of 3-dB cutoff frequencies.

As we can see in Fig. 12, the increase of  $N$  up to 5 enables one to achieve the tuning range of 19.5% that is in line with the results obtained for a single-stub resonator (Fig. 3). The variation of the FBW versus  $N$  does not exceed 2.5%.

Finally, Fig. 13 represents the variation of the central frequency and insertion loss (IL) defined from HFSS simulations versus number of tubes. Here,  $f_1$  and  $f_2$  denote the central frequency of the filter being in 'off' and 'on' states, respectively. The variation of  $f_2$  reveals the impact of empty tubes on the central frequency, whereas  $f_1$  enables one to estimate the tuning range for each value of  $N$ . The insertion loss of the filter remains below 0.6 dB for all  $N$ , that is much lower than reported for tunable filters based on alternative approaches [1]-[10]. Note that tubes can be filled in independently enabling a multi-step tuning of the filter center frequency within a given range with the total number of states equal to  $N+1$ , where  $N$  is the number of tubes.

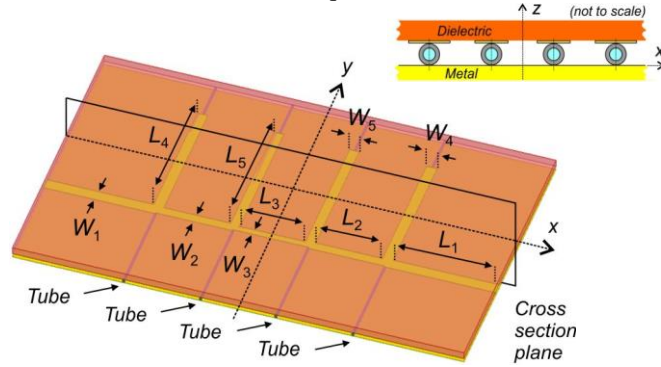
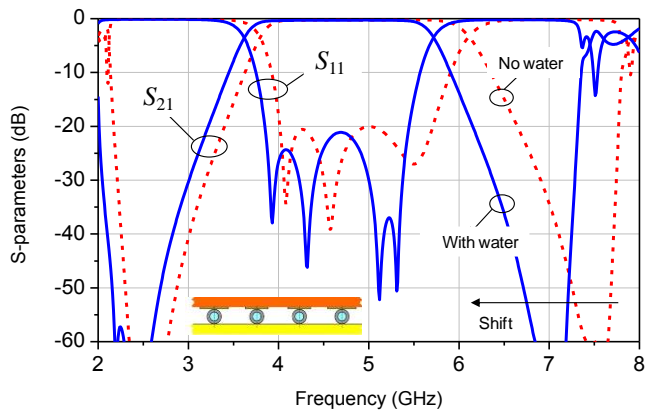


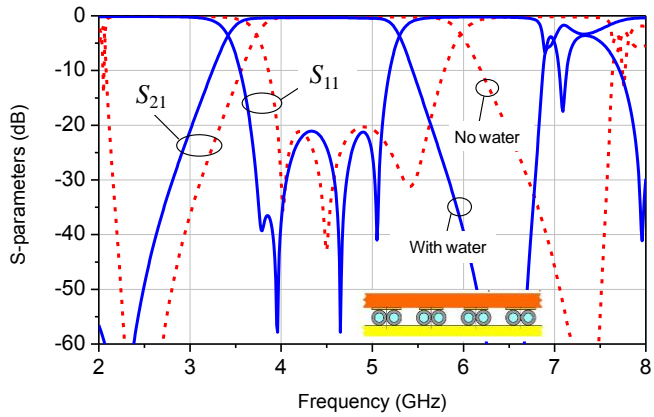
Fig. 10. Topology and notations of the 4th-order microfluidic tunable bandpass filter. The structure is symmetrical with respect to  $yz$ -plane. The substrate size is 90mm $\times$ 55mm.

TABLE I. DIMENSIONS OF THE FILTER (in mm)

$L_1$	$L_2$	$L_3$	$L_4$	$L_5$	$W_1$	$W_2$	$W_3$	$W_4$	$W_5$
Initial values									
22.90	13.15	12.91	13.07	13.01	2.27	1.74	1.19	1.30	1.19
Optimized values									
21.14	13.35	13.11	13.07	13.01	2.27	1.84	1.26	2.07	1.89



(a)



(b)

Fig. 11. Simulated S-parameters of the filter shown in Fig. 10: (a) one tube, (b) two tubes. The blue solid and red dashed lines denote two states of the filter with and without water, respectively.

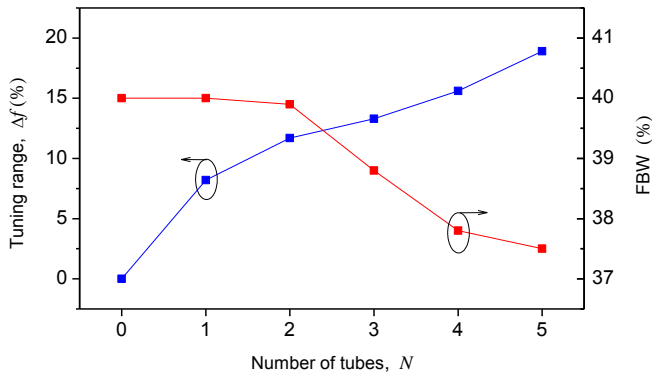


Fig. 12. Shift in central frequency (left axis) and FBW (right axis) of the filter vs. number of tubes.

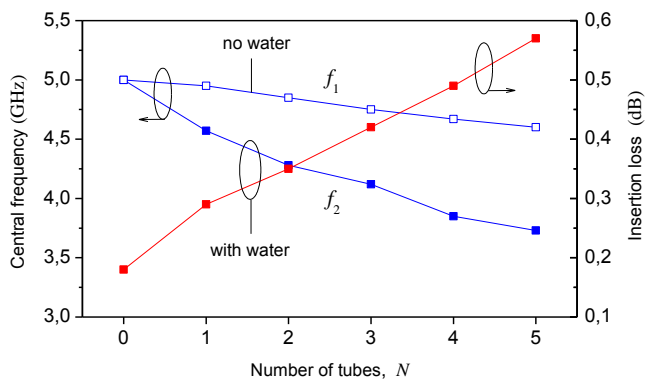


Fig. 13. Central frequency (left axis) and insertion loss (right axis) of the filter vs. number of tubes.

*Experimental data*

A prototype of the proposed microfluidic tunable filter is shown in Fig. 14. Its dimensions are given in Table I (optimal design). It was fabricated using the same technique and materials as the single stub resonator reported in Section II.C.

The measured and simulated S-parameters of the filter with one and two tubes are shown in Fig. 15. A good agreement between the measured and simulated data is achieved both for the FBW and tuning range. A slightly higher level of  $S_{11}$  within the pass band is explained by the cumulative effect of the factors discussed in Section II.C. An additional negative impact on the reflection coefficient is possible due to the SMA connectors soldered to the inverted MS line (their impact is not important for stub resonators because of the performance difference: stopband in case of stubs and passband in case of the filter). The obtained experimental data confirm the feasibility of the proposed approach for the development of more complex microfluidically tunable and reconfigurable devices.

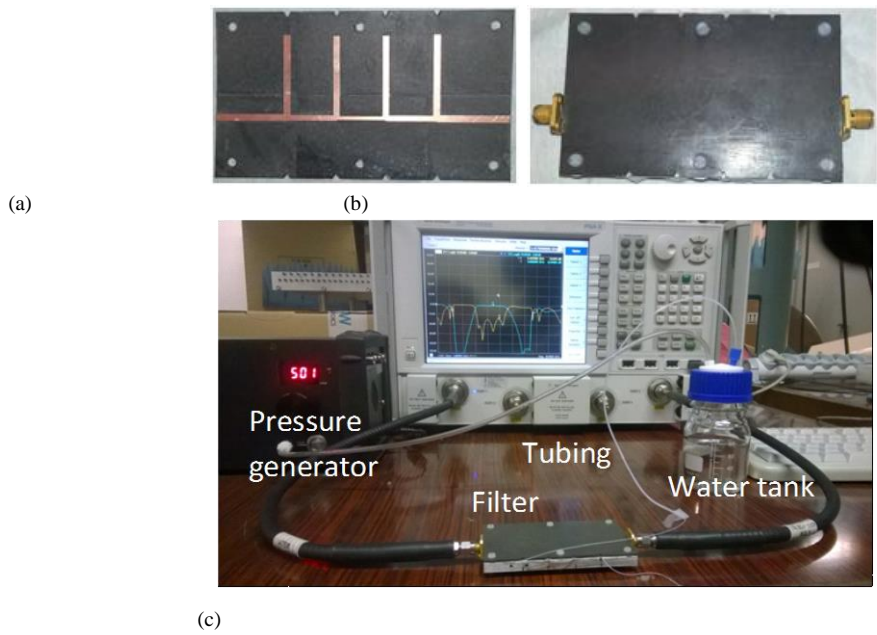
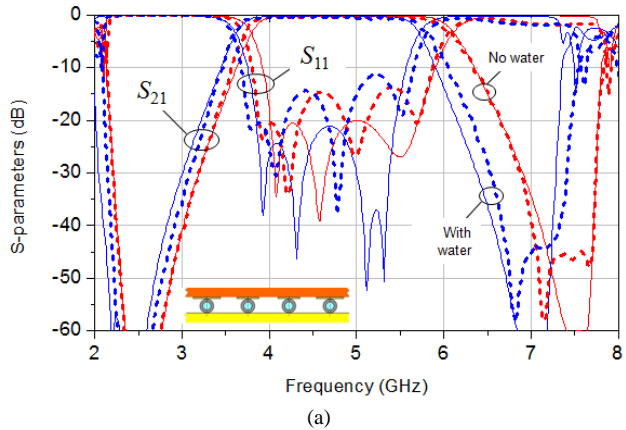


Fig. 14. Prototype of the tunable filter: (a) dielectric substrate with the 4<sup>th</sup> order bandpass filter, (b) assembled device on the aluminum plate with SMA connectors, (c) measurement setup. The dimensions are given in Table I.



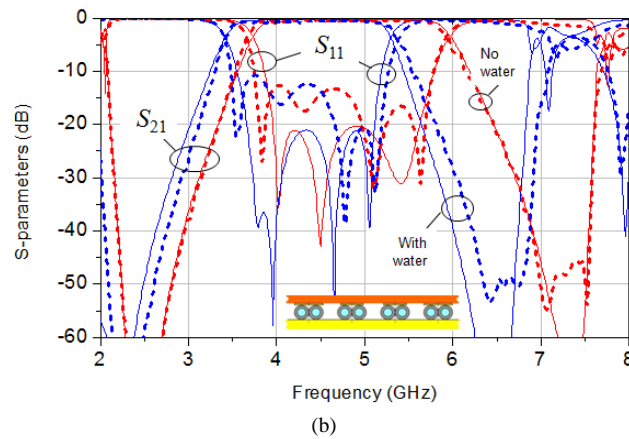


Fig. 15. Measured and simulated  $S$ -parameters of the filter shown in Fig. 10: (a) one tube, (b) two tubes. The blue solid and red dashed lines denote two states of the filter with and without water, respectively.

#### IV. CONCLUSION

A new approach for the development of tunable microstrip filters has been proposed based on the microfluidic principle. The originality of the approach consists in using inverted microstrip lines and plastic tubes oriented parallel to stub resonators. Two types of tunable filters have been designed and fabricated as a proof-of-concept. The performance of microstrip stub resonators, based on suspended and inverted microstrip lines, have been compared. The latter configuration was found more attractive due to a wider tuning range and lower sensitivity to possible misalignment between stubs and microfluidic channels. Then, an UWB bandpass filter with a fractional bandwidth of 40% has been implemented, based on the same approach. Its theoretical tuning range is 19% with the insertion loss of  $<0.6$  dB. A literature review showed that these characteristics are sound compared to existing analogs.

The performance of both devices has been validated successfully via prototyping. The time-domain measurements of the tunable stub resonator revealed reversible switching between two states with a switching time of about 70ms.

The proposed approach can be used for the development of a wide class of tunable and reconfigurable devices. It can be scaled in frequency, subject to a proper account for the frequency dispersion of the fluid permittivity and limitations in feasible dimensions of plastic tubing and suspended structures. Note that in the reported study the tube parameters were not included in optimization which leaves space for further improvements. In particular, the use of tubes with thinner walls and/or rectangular cross-section may help one to increase the tuning range of microfluidic devices, thanks to a more compact arrangement of microfluidic channels.

#### REFERENCES

- [1] E. Fourn, A. Pothier, C. Champeaux, P. Tristant, A. Catherinot, P. Blondy, G. Tanne, E. Rius, C. Person, and F. Huret, "MEMS switchable interdigital coplanar filter," *IEEE Trans. Microw. Theory Techn.*, vol. 51, no. 1, pp. 320–324, Jan. 2003.
- [2] C. L. Goldsmith, A. Malczewski, Z. J. Yao, S. Chen, J. Ehmke, and D.H. Hinzl, "RF MEMS variable capacitors for tunable filters," *Int. J. RF Microw. Computer-Aided Engineering*, vol. 9, no. 4, pp. 362–374, 1999.
- [3] K. Entesari and G. M. Rebeiz, "A 12–18 GHz three-pole RF MEMS tunable filter," *IEEE Trans. Microw. Theory Techn.*, vol. 53, pp. 2566–2571, Aug. 2005.
- [4] F. Mahe, G. Tanne, E. Rius, C. Person, S. Toutain, F. Biron, L. Billonnet, B. Jarry, and P. Guillon, "Electronically switchable dual-band microstrip interdigital bandpass filter for multistandard communication applications," in *Proc. Eur. Microw. Conf. (EuMC)*, Paris, France, Sep. 28–30, 2000.
- [5] B. Kapilevich, "A varactor-tunable filter with constant bandwidth and loss compensation," *Microw. J.*, vol. 50, no. 4, pp. 106–114, Apr. 2007.
- [6] B.-W. Kim and S.-W. Yun, "Varactor-tuned combline bandpass filter using step-impedance microstrip lines," *IEEE Trans. Microw. Theory Techn.*, vol. 52, no. 4, pp. 1279–1283, Apr. 2004.
- [7] I. Vendik, O. Vendik, V. Pleskachev, and A. Svishech, "Design of tunable ferroelectric filters with a constant fractional band width," in *Proc. IEEE MTT-S Int Microw. Symp. Dig.*, Phoenix, AZ, May 20–25, 2001, pp. 1461–1464.
- [8] J. F. Bernigaud, N. Martin, P. Laurent, C. Quendo, G. Tanne, B. Della, F. Huret, and P. Gelin, "Liquid crystal tunable filter based on DBR topology," in *Proc. Eur. Microw. Conf. (EuMC)*, Manchester, UK, Sep. 10–15, 2006, pp. 368–371.
- [9] D. E. Oates, A. Pique, K. S. Harshavardhan, J. Moses, F. Yang, and G. F. Dionne, "Tunable YBCO resonators on YIG substrates," *IEEE Trans. Appl. Supercond.*, vol. 7, no. 2, pp. 2338–2342, Jun. 1997.
- [10] R. Gómez-García, M.-Á. Sánchez-Soriano, K.-W. Tam, and Q. Xue, "Flexible filters," *IEEE Microw. Mag.*, vol. 15, no. 5, pp. 43–54, 2014.
- [11] L. Le Cloirec, A. Benlarbi-Delai, and B. Bocquet, "New concept of RF functions by microfluidic coupling," *Microwave Optical Technol. Lett.*, vol. 48, no. 10, pp. 1912–1916, Oct. 2006.
- [12] S. Pinon, D. L. Diedhiou, A.-M. Gue, N. Fabre, G. Prigent, V. Conedera, E. Rius, C. Quendo, B. Potelon, J.-F. Favennec, and A. Boukabache, "Development of a microsystem based on a microfluidic network to tune and reconfigure RF circuits," *J. Micromechanics and Microengineering*, vol. 22, no. 7, p. 074005, Jul. 2012.
- [13] M. R. Khan, G. J. Hayes, S. Zhang, M. D. Dickey, and G. Lazzi, "A pressure responsive fluidic microstrip open stub resonator using a liquid metal alloy," *IEEE Microw. Compon. Lett.*, vol. 22, no. 11, pp. 577–579, Nov. 2012.
- [14] G. Mumcu, A. Dey, and T. Palomo, "Frequency-agile bandpass filters using liquid metal tunable broadside coupled split ring resonators," *IEEE Microw. Compon. Lett.*, vol. 23, no. 4, pp. 187–189, Apr. 2013.

- [15] O.L. Chlieh, W.T. Khan, and J. Papapolymerou, "L-band tunable microstrip bandpass filter on multilayer organic substrate with integrated microfluidic channel," in *Proc. Int. Microwave Symp. (IMS)*, Tampa Bay, FL, Jun. 1-6, 2014.
- [16] A.P. Saghati, J. Batra, J. Kameoka, and K. Entesari, "Microfluidically-tuned miniaturized planar microwave resonators," in *Proc. IEEE Wireless Microw. Technol. Conf. (WAMICON)*, Jun. 2014, Tampa, FL.
- [17] C.-H. Chen, J. Whalen, and D. Peroulis, "Liquid RF MEMS wideband reflective and absorptive switches," *IEEE Trans. Microwave Theory Techn.*, vol. 55, no. 12, pp. 2919–2929, Dec. 2007.
- [18] P. Sen and C.-J. Kim, "Microscale liquid-metal switches - a review," *IEEE Trans. Ind. Electron.*, vol. 56, no. 4, pp. 1314–1330, Apr. 2009.
- [19] M. Li and N. Behdad, "Fluidically tunable frequency selective/phase shifting surfaces for high-power microwave applications," *IEEE Trans. Antennas Propag.*, vol. 60, no. 6, pp. 2748–2759, Jun. 2012.
- [20] E. Erdil, K. Topalli, Ö. Zorlu, T. Toral, E. Yildirim, H. Kulah, and O.A. Civi, "A reconfigurable microfluidic transmitarray unit cell," in *Proc. Eur. Conf. Antennas Propag. (EuCAP)*, The Hague, The Netherlands, Apr. 6-11, 2014, pp. 2853–2856.
- [21] W. J. Ellison, K. Lamkaouchi, and J.-M. Moreau, "Water: a dielectric reference," *J. Mol. Liq.*, vol. 68, no. 2–3, pp. 171–279, Apr. 1996.
- [22] U. Kaatze, "Complex permittivity of water as a function of frequency and temperature," *J. Chem. Eng. Data*, vol. 34, no. 4, pp. 371–374, 1989.
- [23] J.-S. Hong and M. J. Lancaster, *Microstrip filters for RF/microwave applications*. New York: Wiley, 2001.



**Daouda Lamine Diedhiou** received the MS degree in electronic systems and electrotechnique in 2009 from Nantes Polytech, France, and the Ph.D. degree in electronics from the Université de Bretagne Occidentale (UBO), Brest France within the “Laboratoire des Sciences et Technologies de l'Information, de la Communication et de la Connaissance” (Lab-STICC) in December 2012. Since 2013, he has been working as a postdoctoral researcher at the Institut d'Electronique et de Télécommunication de Rennes (IETR), France. His research activities concern the design of passive functions filters, antennas and phase shifters, providing original solutions in terms of synthesis techniques, analysis and optimization procedures for microwave and millimeter waves applications. He is also concerned with tunable and flexible devices based on liquid metal and soft materials.



**Ronan Sauleau** (M'04–SM'06) graduated in electrical engineering and radio communications from the Institut National des Sciences Appliquées, Rennes, France, in 1995. He received the Agrégation degree from the Ecole Normale Supérieure de Cachan, France, in 1996, and the Doctoral degree in signal processing and telecommunications and the “Habilitation à Diriger des Recherches” degree from the University of Rennes 1, France, in 1999 and 2005, respectively.

He was an Assistant Professor and Associate Professor at the University of Rennes 1, between September 2000 and November 2005, and between December 2005 and October 2009, respectively. He has been appointed as a full Professor in the same University since November 2009. His current research fields are numerical modeling (mainly FDTD), millimeter-wave printed and reconfigurable (MEMS) antennas, substrate integrated waveguide antennas, lens-based focusing devices, periodic and non-periodic structures (electromagnetic bandgap materials, metamaterials, reflectarrays, and transmitarrays) and biological effects of millimeter waves. He has been involved in more than 30 research projects at

the national and European levels and has co-supervised 14 post-doctoral fellows, 24 PhD students and 40 master students.

He has received eight patents and is the author or coauthor of more than 160 journal papers and 360 publications in international conferences and workshops. He has shared the responsibility of the research activities on antennas at IETR in 2010 and 2011. He is now co-responsible for the research Department ‘Antenna and Microwave Devices’ at IETR and is deputy director of IETR. Prof. Sauleau received the 2004 ISAP Conference Young Researcher Scientist Fellowship (Japan) and the first Young Researcher Prize in Brittany, France, in 2001 for his research work on gain-enhanced Fabry-Perot antennas. In September 2007, he was elevated to Junior member of the “Institut Universitaire de France”. He was awarded the Bronze medal by CNRS in 2008. He was the co-recipient of several international conference awards with some of his students (Int. Sch. of BioEM 2005, BEMS'2006, MRRS'2008, E-MRS'2011, BEMS'2011, IMS'2012, Antem'2012). He served as a guest editor for the IEEE Antennas Propagat. Special Issue on “Antennas and Propagation at mm and sub mm waves”.



**Artem V. Boriskin** (M'99, SM'12) was born in Kharkov, Ukraine in 1977. He received the M.S. degree (*cum laude*) in radiophysics and electronics from the Kharkov National University in 1999 and the Ph.D. degree in radiophysics from IRE NASU, Kharkov, Ukraine, in 2004.

In the years 2004–2009, he held positions of a Research Scientist and a Senior Research Scientist at the Department of Computational Electromagnetics of IRE NASU. During these years, he also had short appointments at the Bilkent University (Turkey), IT-Warsaw (Poland), the George Green Institute for Electromagnetics Research, Univ. Nottingham (UK), and IETR (France). Since January 2010, he is with IETR (France) with the department of Antennas and Microwave Devices. His current research interests include computational electromagnetics, integrated lens and corrugated horn antennas for mm-wave applications, planar wearable antennas, bioelectromagnetics, microfluidically tunable microwave devices, and flexible electronics. He is a (co-)author of more than 100 scientific publications.

Dr. Boriskin received several awards including the IEEE MTT-S Graduate Student Fellowship Award in 2000, 1st Microwave Prize from the European Microwave Association in 2004, and 2nd award from the Samsung Corp. in 2005. In 2009, he received a Government Award and the Medal “For the contribution to development of Ukraine”. From the year 2004 to 2008, he was a head of the Young Scientist Council of IRE NASU. In the years 2007–2009, he was a founder and faculty adviser of the student chapter of the Optical Society of America (OSA) at IRE NASU recognized as the best OSA chapter in 2008. In 2009, he also served as a mentor of the IEEE IRE-Kharkov student branch chapter.

In the years 2002–2011, Dr. Boriskin acted as a member of organizing and TPC committees, secretary, and publication chair of multiple national and international conferences, including MMET (2004, 2006, 2008), MSMW (2004, 2007), ICTON (2010), EuMC (2013), and EuCAP (2015). Since 2010, he is a scientific secretary of the ESF Research Networking Program NEWFOCUS dedicated to integrated dielectric focusing systems at mm and sub-mm waves.